CrystEngComm

Accepted Manuscript

ROYAL SOCIETY OF CHEMISTRY

www.rsc.org/crystengcomm

CrystEngComm, Invited paper – IYCr Celebration Theme Issue

Thermal and Photochemical Control of Nitro-Nitrito Linkage Isomerism in Single-Crystals of [Ni(medpt)(NO_2)(η^2-ONO)]†

Lauren E. Hatcher,[a] Edward J. Bigos,[a] Mathew J. Bryant,[a] Emily M. MacCready,[a] Thomas P. Robinson,[a] Lucy K. Saunders,[a] Lynne H. Thomas,[a] Christine M. Beavers,[b] Simon J. Teat,[b] Jeppe Christensen[c] and Paul R. Raithby*[a,c]

[a] *Department of Chemistry, University of Bath, Bath, BA2 7AY, UK*
E-mail: p.r.raithby@bath.ac.uk
[b] *Advanced Light Source, Lawrence Berkeley National Laboratory, Berkeley, CA 947240, USA*
[c] *Research Complex at Harwell, Rutherford Appleton Laboratory, Harwell, Didcot, Oxon, OX11 0FA, UK*

The known complex [Ni(medpt)(η^1-NO_2)(η^2-ONO)] **1** (medpt = 3,3'-Diamino-*N*-methyldipropylamine) crystallises in the monoclinic space group *P2₁/m* with 1.5 molecules in the asymmetric unit with two different η^1-NO_2 ligand environments in the crystal structure. At 298 K the molecule (A) sitting in a general crystallographic site displays a mixture of isomers, 78% of the η^1-NO_2 isomer and 22% of an *endo*-nitrito-(η^1-ONO) form. The molecule (B) sitting on a crystallographic mirror plane adopts the η^1-NO_2 isomeric form exclusively. However, a variable temperature crystallographic study showed that the two isomers were in equilibrium and upon cooling to 150 K the η^1-ONO isomer converted completely to the η^1-NO_2 isomer, so that both independent molecules in the asymmetric unit were 100% in the η^1-NO_2 form. A kinetic analysis of the equilibrium afforded values of $\Delta H = -9.6$ (± 0.4) kJ mol^{-1}, $\Delta S = -21.5$ (± 1.8) J K^{-1} mol^{-1} and $E_A = -1.6$ (± 0.05) kJ mol^{-1}. Photoirradiation of single crystals of **1** with 400 nm light, at 100 K, resulted in partial isomerisation of the η^1-NO_2 isomer to the metastable η^1-ONO isomer, with 89% for molecule (A), and 32% for molecule (B). The crystallographic space group also reduced in symmetry to *P2₁* with *Z'* = 3. The metastable state existed up to a temperature of 150 K above which temperature it reverted to the ground state. An analysis of the crystal packing in the ground and metastable states suggests that hydrogen-bonding is responsible for the difference in the conversion between molecules (A) and (B).

Introduction

The development of photocrystallography,[1] the study of the structures of molecules in photoactivated metastable or excited states using single-crystal X-ray crystallography, has led to the study of a range of chemical processes in the solid-state including cycloaddition reactions,[2] LIESST spin crossover transformations[3] and the determination of the structures of molecular complexes that have transient lifetimes.[4] One of the most fascinating areas of research has been that of solid-state photoactivated linkage isomerism[5] in which ambidentate ligands alter their coordination mode to give a metastable or short-lived species. One of the features common to the solid-state process is that incomplete conversion from one linkage isomer to another occurs and, in the majority of the early cases reported, conversions of less than 50% are observed before a stationary photo-state is reached or crystal degradation occurs.[6] Only in a few cases where the "reaction cavity"[7] around the photoactive ligand has been "engineered" to provide sufficient flexibility have high levels of conversion or, indeed, 100% conversion been observed.[8] If the generation and manipulation of these metastable states is to have any "real-world" applications it is essential to be able to control both the rate and level of conversion. It is already known that the generation of metastable states causes changes in colour, refractive index or non-linear optical properties of solid-state complexes,[9] and we,[10] and others,[5d, 5g] are exploring both steric and kinetic effects that favour the formation of metastable linkage isomers.

The majority of photocrystallographic studies that have been carried out on linkage isomers have been on complexes that contain only one ambidentate ligand or where the ambidentate ligands are related by crystallographic symmetry. A notable exception is the microsecond time-resolved study on [Cu(2,9-dimethyl-1,10-phenanthroline)(1,2-bis(diphenylphosphino)etane)][PF_6] which shows that the two independent copper(I) centres distort to different extents upon photoactivation.[11] The differences were attributed to differences in the crystal environment of the two independent molecules. Thus, it is apparent that the molecular environment within the crystal is important in determining the level of conversion to the short-lived or metastable state. We decided to probe this aspect further by including in our programme of studies on photoactivated nitro-nitrito interconversions[5a, 12] by carrying out a photocrystallographic study on [Ni(medpt)(η^1-NO_2)(η^2-ONO)][13] (medpt = 3,3'-Diamino-*N*-methyldipropylamine). The system crystallises in the monoclinic space group $P2_1/m$ with one-and-a-half molecules in the asymmetric unit and has η^1-NO_2 ligand environments that have different symmetry restraints. We now report the results of this study.

Results and discussion

*Crystal structure of [Ni(medpt)(η^1-NO_2)(η^2-ONO)] **1** at 298 K*

The complex [Ni(medpt)(η^1-NO_2)(η^2-ONO)] **1** was prepared by literature methods[13] and obtained as violet crystals by evaporation from methanol. The crystal structure was re-determined initially at 298 K. The complex crystallises in the monoclinic space group $P2_1/m$ with 1.5 molecules in the asymmetric unit. The molecular structures of the two unique molecules are illustrated in Fig. 1. While molecule (A) occupies a general position, molecule (B) is located on the mirror plane such that the mirror bisects Ni(2), N(11), N(12), N(14), O(13), O(14) and C(17). As such there is a 2:1 ratio of (A) to (B) molecules in the crystal. Both nickel centres are six-coordinate, bound to one monodentate nitrite, one nitrito-(η^2-O,ON) group and one tridentate amine ligand. Although identical in their constituent components, the two independent molecules are in fact geometric isomers of one another. In molecule (A) the amine binds meridionally such that the *N*-methyl substituent points downwards away from the monodentate nitrite. However in molecule (B) the amine, though also meridionally coordinated, is inverted such that its *N*-methyl group points upwards towards the nitrite. This geometric difference was not identified in the original study,[13] but it provides an explanation as to why the two molecules must adopt crystallographically distinct environments. The monodentate nitrite ligand adopts nitro-(η^1-NO_2) geometry as the major form in both species and, while this is the sole isomer present for molecule (B), in molecule (A) a minor *endo*-nitrito-(η^1-ONO) component is also identified at 22%.

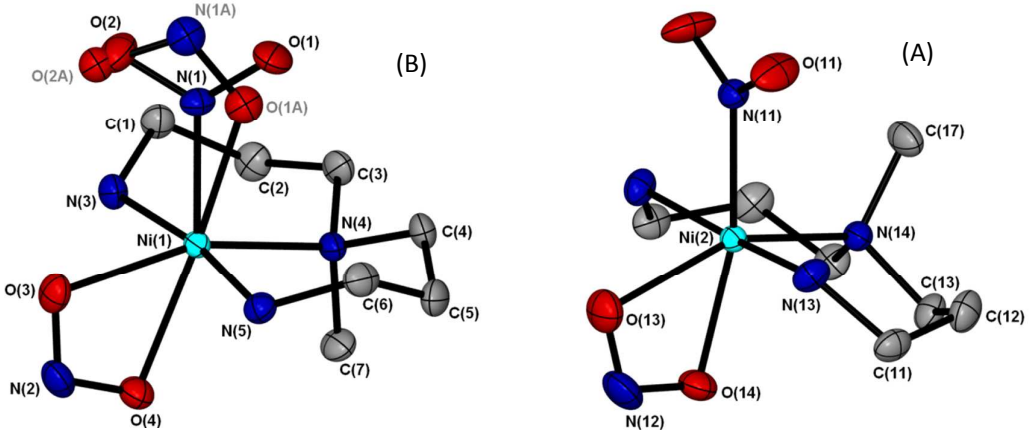

Figure 1. Molecular structures for the two independent molecules of **1** at 298 K, molecule (A) (right) situated on a general position and molecule (B) (left) situated at a mirror plane. Hydrogen atoms removed for clarity.

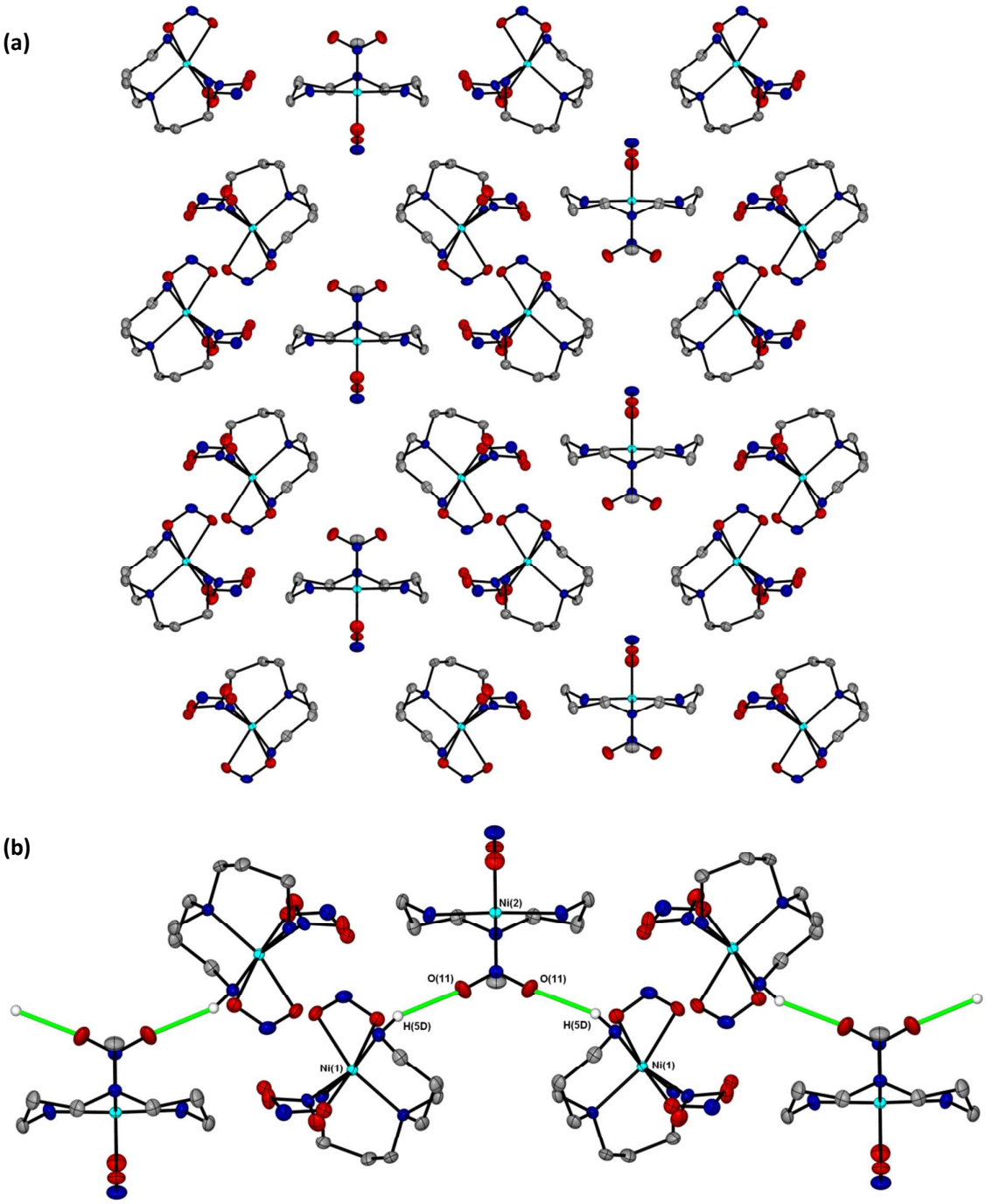

Figure 2. (a) Crystal packing arrangement for the structure of **1** at 298 K, **(b)** hydrogen bonding interactions to the nitro-(η^1-NO_2) ligand in molecule (B).

The crystal packing for **1** is illustrated in Fig. 2. Molecules of the same isomer align in rows along the *a*-axis (into the plane of the paper in Fig. 2) and there are no significant interactions between the molecules within each row. The symmetry-related nitro oxygen atoms O(21) of molecule (B) are involved in a N(5)-H(5D)…O(11) contact to a neighbouring molecule (A). This creates hydrogen bond chains throughout the structure, involving both species and running parallel to the *b*-axis. By contrast, there are no hydrogen bonds involving the nitrite in molecule (A) and these are oriented away from the bulky amine groups.

Variable Temperature studies

Given that a thermal equilibrium between the nitro and nitrito isomers had been observed previously in the complex [Ni(Et_4dien)(NO_2)$_2$],[14] the structure of **1** was determined at intervals over the temperature range 100 – 298 K to assess the effect of temperature on the nitro : nitrito ratio in molecule (A). In this procedure the crystal was slowly cooled from 298 to 100 K, *in-situ* on the diffractometer and in the absence of light. Cooling was paused at regular intervals to allow collection of a full single-crystal X-ray dataset, from which the nitro : nitrito isomer ratio for molecule (A) was then refined at each temperature. The crystal was held at each stage for 5 min to allow the temperature to equilibrate, before a new experiment was conducted. The results of the study are presented in Table 1. Molecule (B) showed no change in coordination of the nitro group with temperature reflecting the differing intermolecular interactions of the two molecules.

Table 1. Crystallographically determined nitro : nitrito ratios for molecule (A) of **1** as a function of temperature on cooling

Temp / K	Molecule A - Occupancy (esd)	
	Nitro-(η^1-NO_2)	Nitrito-(η^1-ONO)
298	0.78(1)	0.22(1)
250	0.89(1)	0.11(1)
200	0.96(1)	0.04(1)
150	1[a]	0[a]
100	1[a]	0[a]

[a] No esd is reported for full occupancy or zero occupancy as these ratios were not refined

The nitro : nitrito ratio was observed to change on cooling, with conversion to the nitro-(η^1-NO_2) isomer increasing as the temperature was lowered. By 150 K no evidence of the *endo*-nitrito-(η^1-ONO) isomer could be found in difference maps, confirming that a 100% nitro isomer had been achieved on cooling. As for [Ni(Et_4dien)(NO_2)$_2$],[14] this result indicates the two linkage isomers exist in a thermodynamic equilibrium at ambient temperature and the position of this equilibrium can be shifted by varying the temperature. The nitro-(η^1-NO_2) isomer appears to be the more thermodynamically stable arrangement, as it is preferred at low temperature.

Although only limited data were obtained in this variable temperature experiment, it was possible to perform a kinetic analysis of the equilibrium. A Van't Hoft plot was constructed for the data between 298 - 200 K and used to approximate thermodynamic data using Equn 1.

$$(-R)\ln(K_{eq}) = \Delta H\left(\frac{1}{T}\right) - \Delta S \qquad \text{Equation 1}$$

The Van't Hoft plot (Fig. 3) shows good linear regression, with R^2 = 0.996. The negative slope confirms the nitro-(η^1-NO_2) isomer is enthalpically favoured by ΔH = –9.6 (± 0.4) kJ mol^{-1}, while a value of ΔS = –21.5 (± 1.8) J K^{-1} mol^{-1} is obtained for the entropy change on nitrito – nitro conversion. These values are comparable to those obtained for [Ni(Et_4dien)(NO_2)$_2$].[14]

An Arrhenius plot was also constructed, allowing an estimate of the activation energy E_A for the thermal isomerisation process to be made. The plot, presented in Fig. 4, again shows good linear correlation between Equn. 2 and the data, returning an estimation of E_A = –1.6 (± 0.05) kJ mol^{-1}. This value is smaller than that obtained for [Ni(Et_4dien)(NO_2)$_2$],[14] but is still comparable. The values for ΔH, ΔS and E_A are indicative of a low energy barrier between the isomers, suggesting they are close in energy. This is to be expected since both isomers co-exist in the crystal under ambient conditions.

$$ln(K_{eq}) = -E_A\left(\frac{1}{RT}\right) + \ln(A) \qquad \text{Equation 2}$$

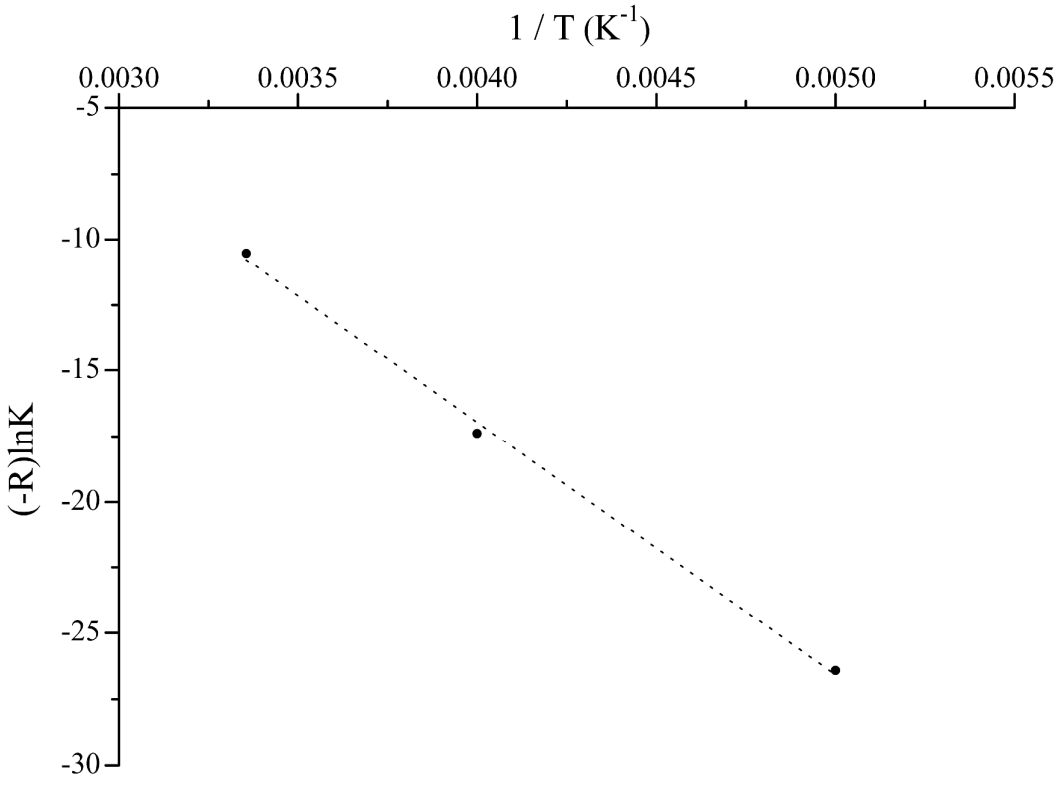

Figure 3. Van't Hoft plot for the thermodynamic equilibrium in **1**. Slope m = standard enthalpy (ΔH) = –9.6 (± 0.4) kJ mol^{-1}, intercept C = entropy (ΔS) = –21.5 (± 1.8) J K^{-1} mol^{-1}, R^2 = 0.996.

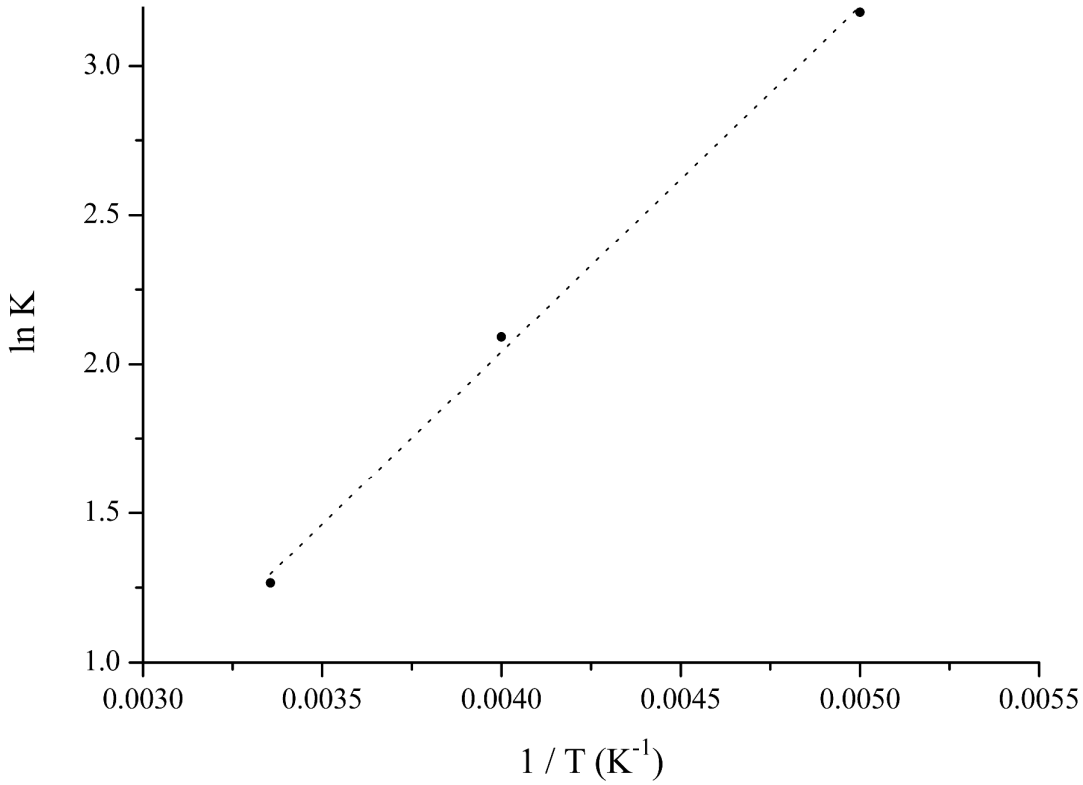

Figure 4. Arrhenius plot for the thermally induced isomerisation reaction in **1**. Activation energy E_A = –1.16 (± 0.05) kJ mol^{-1}, R^2 = 0.996.

Steady-state photocrystallography

The UV/visible spectrum of **1** exhibited a dominant absorption at 361 nm (see Supporting Information). This is characteristic of a MLCT transition and irradiation in the tail of this absorption band would be appropriate for generating a metastable linkage isomer.[15]

A crystal of **1** was first slow cooled to 100 K, in the dark, to ensure both molecules (A) and (B) adopt the 100% nitro-(η^1-NO_2) linkage isomer arrangement in the ground state (GS). The crystal was then irradiated with 400 nm LED light at 100 K for a period of 1 h, *in-situ on the diffractometer* using a specifically designed LED ring array. This experimental set up has been described previously[16] and positions six LEDs in a ring *c.a.* 1 cm from the crystal position. The crystal was also rotated during this period, helping to further ensure uniform illumination. After the irradiation period, a second X-ray dataset was then collected in the absence of further light. This dataset revealed that a change in both molecules is induced on excitation. Whilst 89% conversion to a nitrito-(η^1-ONO) isomer had been achieved for molecule (A), a minor 32% nitrito isomer was also identified for molecule (B). Linkage isomerism in molecule (B) necessarily breaks the mirror symmetry required at this site in $P2_1/m$. The *N*-methyl group, C(17), also breaks the original symmetry, preferring to sit just off the mirror plane in the metastable state (MS) structure (Fig. 5). Given the asymmetric arrangement for the *endo*-nitrito excited state (ES), refinement in the original centrosymmetric space group $P2_1/m$ does not sufficiently describe the MS structure of (B). It is not possible to adequately model the disorder across the mirror plane and, most importantly, to obtain a value for the MS conversion level in the molecule. As such, a more satisfactory model was obtained in $P2_1$. The reduction in symmetry raises the number of molecules in the asymmetric unit to $Z' = 3$ and, as only molecule (B) breaks the symmetry of the original GS cell, the other two molecules are essentially similar. This is confirmed by the fact that they are the same geometric isomer (molecule (A), Fig. 5) and their nitro : nitrito ratios refine to similar values. As such conversion levels reported for molecule A are an average over the two, now assigned as molecules (A) and (A'). Apart from the photoexcited components of molecule (B), the majority of the ES structure still obeys the symmetry constraints of the GS space group $P2_1/m$, approximately, it is unsurprising that refinement in the lower symmetry space group requires a TWIN instruction. This treatment returns a value for the Flack parameter of *c.a.* 0.5 in all photoexcited datasets modelled in $P2_1$.

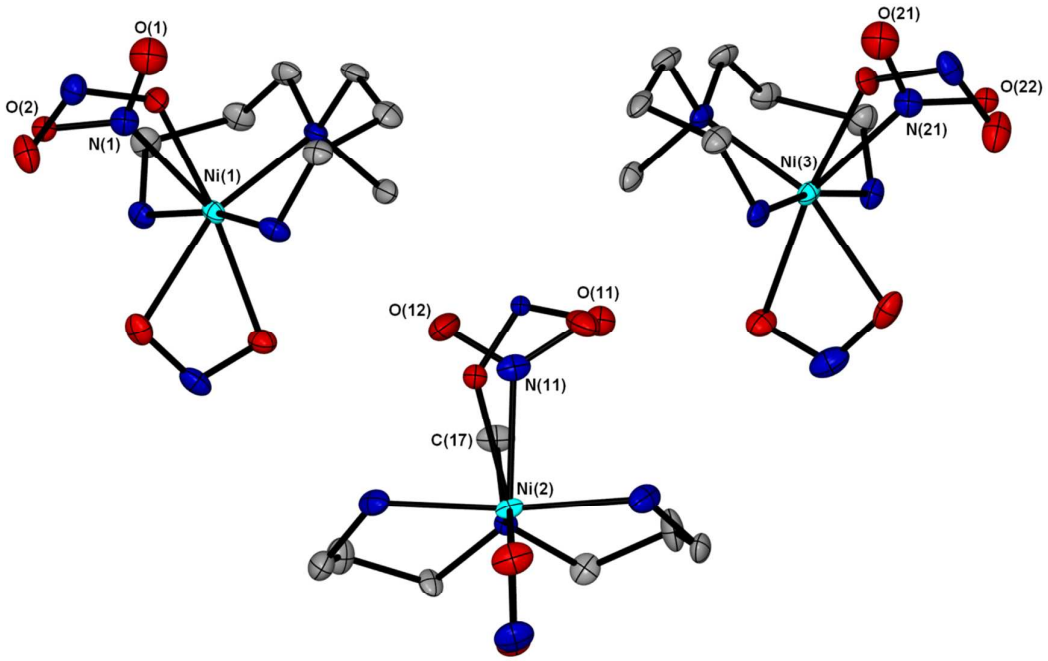

Figure 5. Single-crystal X-ray structure showing the atomic arrangement for the three independent molecules in the metastable state structure of **1**. Hydrogen atoms omitted for clarity.

No further change in the excitation level for any of the molecules could be induced on further irradiation, confirming that a photostationary state had been achieved. The MS structure remained constant on holding the crystal at 100 K in the dark, confirming it to be metastable under the experimental conditions.

Variable temperature parametric studies were then conducted to determine the temperature range over which the photoactivated state is metastable. The nitrito isomers in both molecules remain constant on warming to 110 K, but begin to decrease on further heating. By 150 K molecule (B) has regained its GS arrangement and the structure is now best solved in the original $P2_1/m$ unit cell. On further warming the nitrito isomer occupancy in molecule (A) continues to decrease, until at 135 K this molecule also returns to the GS nitro-(η^1-NO_2) arrangement. The nitro : nitrito ratios refined from all photocrystallographic data for molecules (A) and (B) are presented in Table 2.

Table 2: Crystallographically determined nitro : nitrito ratios as a function of exposure to 400 nm LED light during steady-state photocrystallographic experiments with **1**

Irradiation time / hr	Temp / K	Molecule A Occupancy[a]		Molecule B Occupancy	
		Nitro-(η^1-NO_2)	Nitrito-(η^1-ONO)	Nitro-(η^1-NO_2)	Nitrito-(η^1-ONO)
0	100	1[b]	0[b]	1[b]	0[b]
1	100	0.11(1)	0.89(1)	0.68(1)	0.32(1)
2	110	0.12(1)	0.88(1)	0.68(1)	0.32(1)
2	115	0.14(1)	0.86(1)	0.70(1)	0.30(1)
2	120	0.25(1)	0.75(1)	0.84(1)	0.16(1)
2	125	0.57(1)	0.43(1)	1[b]	0[b]
2	130	0.92(1)	0.08(1)	1[b]	0[b]
2	135	1[b]	0[b]	1[b]	0[b]

[a] The occupancy is now the average for the two independent molecules A and A'

[b] No esd is reported for full occupancy or zero occupancy as these ratios were not refined

Crystal packing and steric effects

The crystal packing for **1** is largely unchanged on excitation and similar to that shown in Fig. 2, excepting the change in nitrite coordination for molecule (B) and the concomitant reduction in symmetry. The lack of strong intermolecular interactions to molecule (A) could suggest why a mix of linkage isomers is only found for this molecule. Despite the space group change the data in Table 3 confirm there is no dramatic shift in cell parameters, although a small +16(3) $Å^3$ (0.9%) increase in cell volume is observed on excitation that is just significant in terms of the esds.

Table 3. Crystal data for the flash cooled GS and photoinduced metastable structures of **1**, at 100 K

	Ground State	**400 nm Metastable State**
Photoconversion	Molecule A = 0%, B = 0%	Molecule A = 89%, B = 32%
Temperature	100(2) K	100(2) K
Wavelength	0.71073 Å	0.71073 Å
Empirical formula	$C_7 H_{19} N_5 Ni_1 O_4$	$C_7 H_{19} N_5 Ni_1 O_4$
Formula weight	443.97	443.97
Crystal size	0.50 x 0.40 x 0.10 mm^3	0.50 x 0.40 x 0.10 mm^3
Crystal system	Monoclinic	Monoclinic
Space group	$P2_1/m$	$P2_1$
Unit cell dimensions	a = 7.119(5) Å b = 23.688(5) Å β = 103.360(5)° c = 10.909(5) Å	a = 7.100(5) Å b = 23.968(5) Å β = 103.945(5)° c = 10.935(5) Å
Volume	1790(2) $Å^3$	1806(2) $Å^3$
Z	6	6
Density (calculated)	1.648 M g m^{-3}	1.633 M g m^{-3}
Absorption coeff. μ	1.639 mm^{-1}	1.625 mm^{-1}
F(000)	936	936
R(int)	0.0229	0.0398
R1 (obs. data)	0.0251	0.0328
wR2 (all data)	0.0607	0.0753
Reflections (indep.)	5590	7582

As noted in the earlier variable temperature studies, the hydrogen bond network observed in **1** could provide an explanation for the considerably lower photoconversion level achieved for molecule (B). Hydrogen bond data for the GS and MS are given in the Supporting Information. Several intermolecular hydrogen bonds are rearranged following photoconversion in **1**. No hydrogen bonds to the nitrite ligand exist in the GS arrangement for molecule (A), suggesting it is better placed to undergo isomerisation as there are fewer strong contacts providing a barrier to conversion. However, excitation to the nitrito isomer creates new intermolecular hydrogen bonds involving these groups in molecules (A) and (A') (Fig. 6). Formation of these new, weak interactions will be energetically favourable and so should favour the formation of the metastable nitrito-(η^1-ONO) isomer in both cases.

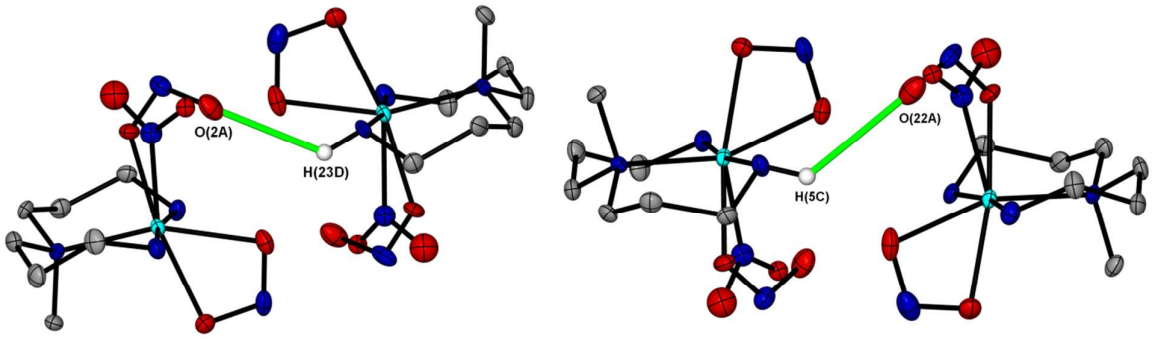

Figure 6. New intermolecular hydrogen bonds formed in the metastable nitrito-(η^1-ONO) form in molecule (A) and (A').

Additionally, the nitrite ligand in molecule (B) is constrained in the GS by two symmetry-related N(5)-H(5D)…O(11) contacts, becoming bonds N(23)-H(23C)…(O11) and N(5)-H(5D)…O(12) when the mirror symmetry is lost upon excitation (Fig. 7, left). These must be broken for isomerisation to occur and in their place a new intermolecular N(23)-H(23A)…(O12A) hydrogen bond to the nitrito isomer must additionally be formed (Fig. 7, right). The breaking and re-forming of these bonds requires extra energy, making conversion in molecule (B) less favourable.

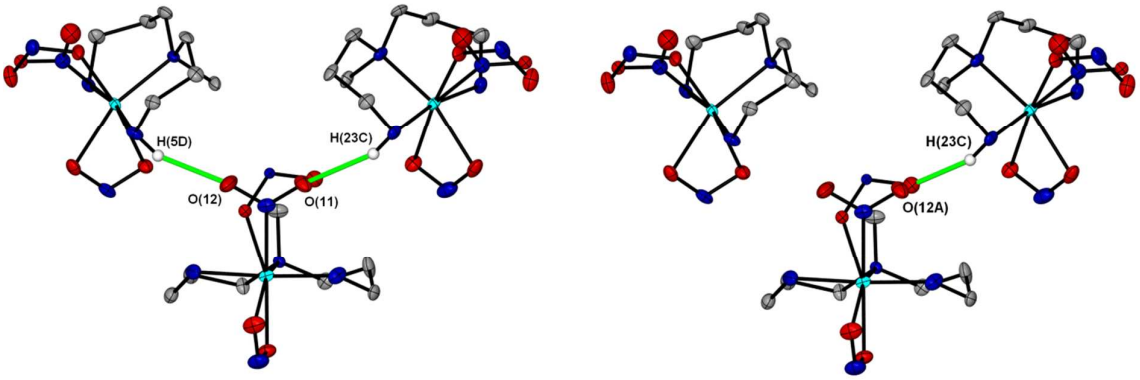

Figure 7. Changes in intermolecular hydrogen bonding to the nitrite in molecule B on excitation

Hirshfeld surfaces were constructed separately around molecules (A) and (B) in turn, such that fingerprint plots could be generated for each of these geometric isomers individually (Supporting Information). Firstly, the overall plots are significantly different for molecules (A) and (B), confirming that they occupy quite different environments within the crystal. Considering each molecule individually, the overall plot shapes are similar for GS and MS, confirming there is little change in the overall structure on excitation. For both molecules (A) and (B), only three key types of interaction contribute to the fingerprint plot: while N…H and O…H contacts must include changes involving the nitrite groups, H…H close contacts will solely represent the rest of the structure. Both the N…H and O…H plots display sharp, spike features that represent hydrogen bonding.[17] For molecule (A), a subtle increase in these features is observed on moving to the MS reflecting the formation of new hydrogen bonds to the metastable nitrito ligands while none exist to the GS nitro isomer, as discussed previously. For molecule (B), a difference between GS and MS contacts is also evident and in particular the formation of a single, shorter O…H hydrogen bond is observed, comparing well with the observations described by Fig. 7. By contrast, the H…H plots for both molecules show little change between GS and metastable state, again confirming that the key differences are only the result of the photochemical linkage isomerisation.

Finally, it has been shown that analysis of the reaction cavity, defined as the region encompassing the photoactive part of the molecule, can be used to rationalise the progress of photoreactions in the solid-state.[18] In the context of **1**, the reaction cavity is defined as the region encapsulating a photoactive nitrite group. The cavity volume can be determined by removing the nitrite ligand in question from the crystal structure and conducting a void space calculation on the remaining structure, using the CCDC software package Mercury.[19] No void space was found to be present in any of the structures of **1** before the removal of the photoactive fragment. Using a contact surface calculation with a probe radius of 1.2 Å and a grid spacing of 0.1 Å, reaction cavity volumes were determine for molecules (A) and (B) in both the GS and MS structures (Table 4). To ensure fair comparison between all molecules, cavity volumes are given as a percentage of the overall cell volume and are additionally normalised by the number of that molecule in the unit cell (*i.e.* divided by 3 for molecule (A) and by 2 for molecule (B), given the 2:1 ratio of (A) to (B)).

Table 4. Reaction cavity volumes encapsulating the nitrite ligands for **1** showing the changes in the photoactive region on excitation.

	Molecule (A) / % of unit cell	Molecule (B) / % of unit cell
Ground State	2.10	1.05
Metastable State	2.17	0.95
ΔV_c	0.07	-0.10

The reaction cavity volume is calculated to be considerably larger for molecule (A) than for molecule (B). Additionally, while ΔV_c, the change in reaction cavity volume on photoactivation, is found to increase for molecule (A), a decrease is observed for molecule (B). This indicates there is less space for nitro – nitrito rearrangement to occur in molecule (B) and, in fact, the amount of available space is further reduced on photoactivation. Both of these factors can provide an additional explanation for the difference in photoconversion level achieved at each site.

Conclusions

The observation that [Ni(medpt)(η^1-NO_2)(η^2-ONO)] **1** does not undergo complete conversion under similar photoreaction conditions to those observed for related nickel(II) complexes[8a, 10a, 14] indicates that solid-state effects must strongly influence the photoreaction, and comparison may suggest the degree to which the crystalline environment can affect the level of achievable photoconversion. In **1** the two independent molecules undergo significantly different levels of conversion when the photostationary state is reached.

The simplest parameter for comparison is first the overall change in unit cell volume ΔV on photoactivation. Generally, the solid-state photoreactions proceed topochemically,[20] therefore the system undergoing the smallest change is necessarily expected to achieve highest photoconversion. For all nitro – nitrito systems so far studied ΔV is small and the overall crystal structure does not change greatly on excitation,[5a] observations consistent with the topochemical postulate. However, the relative changes in ΔV are hardly significant, suggesting that this parameter alone does not effectively account for the trends observed.

However, it is apparent that the degree of hydrogen bonding to the nitrite affects the level of achievable isomerisation. The highest converting species, [Ni(dppe)Cl(NO_2)][8a] and molecule A of **1**, show no intermolecular hydrogen bonding to the nitrite ligand in the ground state. It is expected that for conversion to occur strong hydrogen-bonds in the ground state are best avoided. For molecule B in **1**, the hydrogen-bonding in the ground state is significant, consistent with a lower level of conversion. In contrast, the formation of hydrogen-bonds in the metastable state, as is observed for both molecules A and B in **1**, would help to stabilise this form. Thus, from this study, the clearest influence on the interconversion process would seem to be the competition between the breaking of hydrogen-bonding networks in the ground state and the formation of hydrogen bonding networks in the metastable state.

Experimental

General

The synthesis of **1** was based on literature methods.[13] All chemicals were purchased from commercial sources and used as received. All reactions were performed under an atmosphere of dry nitrogen, however, workup was completed in air. IR spectra were recorded as CH_2Cl_2 solutions in a NaCl cell on a Nicolet-Impact 400D FT-IR spectrometer.

Crystallography

X-ray data for **1** was collected on an Agilent Technologies Gemini A-Ultra diffractometer fitted with an Atlas CCD detector, using Mo-K_α radiation, and equipped with an Agilent Technologies Cryojet

crystal cooling apparatus. For the photocrystallographic experiments sample illumination was achieved by using six 400 nm LEDs (1200 mcd, 3.5 V, 20 mA), positioned 1 cm from the crystal. A Bruker Apex II diffractometer using synchrotron radiation (λ = 0.7749 Å) at Station 11.3.1 of the ALS Lawrence Berkeley National Laboratory was used to collect preliminary single crystal data for the variable temperature kinetic studies, and these measurements were then repeated for consistency using the Agilent Technologies Gemini A-Ultra diffractometer. For the Gemini data the program CrysAlis Pro was used for collecting the frames of data, indexing reflections and determining lattice parameters. The structure was solved by direct methods using *SHELXS-97* and refined by full-matrix least-squares of F^2 using *SHELXL-97*.[21] In the structures above temperatures of 150 K and in the photocrystallographic experiments the η^1-NO_2 and the η^1-ONO contributions were treated as a disorder model, allowing the occupancies to refine freely using free variables in *SHELXL-97*, but with the total occupancy summed to unity. Refinement was continued in each case until convergence was reached. Hydrogen atoms were placed in idealised positions and were allowed to ride on the relevant carbon atom also with isotropic displacement parameters related to the U_{equiv} displacement parameter of the carbon (x 1.2 for methylene H atoms and x 1.5 for methyl H atoms).

Acknowledgements

We are grateful to the EPSRC for financial support for the project (EP/I01974X, EP/F021151 and EP/K004956) and for a studentship to T.P.R. (EP/G067759). We acknowledge the support from University of Bath through studentships for L.E.H. and M.J.B., and the Diamond Light Source Ltd for a studentship to L.K.S. We would also like to thank the ALS, LBNL for beamtime to perform the kinetic experiments. The Advanced Light Source is supported by the Director, Office of Science, Office of Basic Energy Sciences, of the U.S. Department of Energy under Contract No. DE-AC02-05CH11231. Additional thanks goes to COMPRES, the Consortium for Materials Properties Research in Earth Sciences under NSF Cooperation Agreement EAR 11-57758.

Notes and references

†Electronic supplementary information available: Details of all X-ray diffraction and spectroscopic experimental studies. CCDC 994148-994159. For ESI and crystallographic data in CIF or other format see DOI:xx.xxxx/c3cexxxxxn

1. a) P. Coppens, D. V. Fomitchev, M. D. Carducci and K. Culp, *J. Chem. Soc.-Dalton Trans.*, 1998, 865-872; b) P. Coppens, Vorontsov, II, T. Graber, M. Gembicky and A. Y. Kovalevsky, *Acta Crystallogr. Sect. A*, 2005, **61**, 162-172; c) P. Coppens, J. Benedict, M. Messerschmidt, I. Novozhilova, T. Graber, Y. S. Chen, I. Vorontsov, S. Scheins and S. L. Zheng, *Acta Crystallogr. Sect. A*, 2010, **66**, 179-188; d) P. Naumov, in *Advanced X-Ray Crystallography*, ed. K. Rissanen, Editon edn., 2012, vol. 315, pp. 111-131; e) J. M. Cole, *Acta Crystallogr. Sect. A*, 2008, **64**, 259-271.
2. a) T. Friscic and L. R. MacGillivray, *Z. Kristall.*, 2005, **220**, 351-363; b) T. Friscic and L. R. MacGillivray, *Chem. Commun.*, 2005, 5748-5750; c) G. K. Kole, R. Medishetty, L. L. Koh and J. J. Vittal, *Chem. Commun.*, 2013, **49**, 6298-6300; d) M. F. Mahon, P. R. Raithby and H. A. Sparkes, *Crystengcomm*, 2008, **10**, 573-576; e) J. A. K. Howard, M. F. Mahon, P. R. Raithby and H. A. Sparkes, *Acta Crystallogr. Sect. B-Struct. Sci.*, 2009, **65**, 230-237.
3. a) M. A. Halcrow, *Chem. Soc. Rev.*, 2008, **37**, 278-289; b) G. A. Craig, J. Sanchez Costa, O. Roubeau, S. J. Teat, H. J. Shepherd, M. Lopes, G. Molnar, A. Bousseksou and G. Aromi, *Dalton Trans.*, 2014, **43**, 729-737; c) G. A. Craig, J. S. Costa, O. Roubeau, S. J. Teat, H. J. Shepherd, M. Lopes, G. Molnar, A. Bousseksou and G. Aromi, *Dalton transactions (Cambridge, England : 2003)*, 2013, **43**, 729-737; d) K. Katayama, M. Hirotsu, I. Kinoshita and Y. Teki, *Dalton Trans.*, 2012, **41**, 13465-13473.

4. a) P. Coppens, Vorontsov, II, T. Graber, A. Y. Kovalevsky, Y. S. Chen, G. Wu, M. Gembicky and I. V. Novozhilova, *J. Am. Chem. Soc.*, 2004, **126**, 5980-5981; b) P. Coppens, O. Gerlits, Vorontsov, II, A. Y. Kovalevsky, Y. S. Chen, T. Graber, M. Gembicky and I. V. Novozhilova, *Chem. Commun.*, 2004, 2144-2145; c) A. Makal, J. Benedict, E. Trzop, J. Sokolow, B. Fournier, Y. Chen, J. A. Kalinowski, T. Graber, R. Henning and P. Coppens, *J. Phys. Chem. A*, 2012, **116**, 3359-3365.
5. a) L. E. Hatcher and P. R. Raithby, *Acta Crystallogr. Sect. C-Cryst. Struct. Commun.*, 2013, **69**, 1448-U1135; b) M. R. Warren, S. K. Brayshaw, L. E. Hatcher, A. L. Johnson, S. Schiffers, A. J. Warren, S. J. Teat, J. E. Warren, C. H. Woodall and P. R. Raithby, *Dalton Trans.*, 2012, **41**, 13173-13179; c) S. K. Brayshaw, T. L. Easun, M. W. George, A. M. E. Griffin, A. L. Johnson, P. R. Raithby, T. L. Savarese, S. Schiffers, J. E. Warren, M. R. Warren and S. J. Teat, *Dalton Trans.*, 2012, **41**, 90-97; d) S. O. Sylvester and J. M. Cole, *Journal of Physical Chemistry Letters*, 2013, **4**, 3221-3226; e) J. M. Cole, K. F. Bowes, I. P. Clark, K. S. Low, A. Zeidler, A. W. Farker, I. R. Laskar and T. M. Chen, *Cryst. Growth Des.*, 2013, **13**, 1826-1837; f) S. O. Sylvester, J. M. Cole and P. G. Waddell, *J. Am. Chem. Soc.*, 2012, **134**, 11860-11863; g) A. E. Phillips, J. M. Cole, T. d'Almeida and K. S. Low, *Inorg. Chem.*, 2012, **51**, 1204-1206; h) K. F. Bowes, J. M. Cole, S. L. G. Husheer, P. R. Raithby, T. L. Savarese, H. A. Sparkes, S. J. Teat and J. E. Warren, *Chem. Commun.*, 2006, 2448-2450; i) A. Y. Kovalevsky, K. A. Bagley, J. M. Cole and P. Coppens, *Inorg. Chem.*, 2003, **42**, 140-147; j) A. Y. Kovalevsky, K. A. Bagley and P. Coppens, *J. Am. Chem. Soc.*, 2002, **124**, 9241-9248; k) D. V. Fomitchev, I. Novozhilova and P. Coppens, *Tetrahedron*, 2000, **56**, 6813-6820; l) D. V. Fomitchev, K. A. Bagley and P. Coppens, *J. Am. Chem. Soc.*, 2000, **122**, 532-533.
6. a) J. M. Cole, *Analyst*, 2011, **136**, 448-455; b) P. R. Raithby, *Crystallography Reviews*, 2007, **13**, 121-142; c) D. Schaniel, T. Woike, N. R. Behrnd, J. Hauser, K. W. Kramer, T. Todorova and B. Delley, *Inorg. Chem.*, 2009, **48**, 11399-11406.
7. a) P. Naumov and Y. Ohashi, *Acta Crystallogr. Sect. B-Struct. Sci.*, 2004, **60**, 343-349; b) Y. Ohashi, *Crystallography Reviews*, 2013, **19**, 2-146.
8. a) M. R. Warren, S. K. Brayshaw, A. L. Johnson, S. Schiffers, P. R. Raithby, T. L. Easun, M. W. George, J. E. Warren and S. J. Teat, *Angew. Chem.-Int. Edit.*, 2009, **48**, 5711-5714; b) D. Schaniel, N. Mockus, T. Woike, A. Klein, D. Sheptyakov, T. Todorova and B. Delley, *Phys. Chem. Chem. Phys.*, 2010, **12**, 6171-6178; c) B. Cormary, I. Malfant, M. Buron-Le Cointe, L. Toupet, B. Delley, D. Schaniel, N. Mockus, T. Woike, K. Fejfarova, V. Petricek and M. Dusek, *Acta Crystallographica Section B*, 2009, **65**, 612-623.
9. J. M. Cole, *Z. Kristall.*, 2008, **223**, 363-369.
10. a) L. E. Hatcher, J. Christensen, M. L. Hamilton, J. Trincao, D. R. Allan, M. R. Warren, I. P. Clarke, M. Towrie, D. S. Fuertes, C. C. Wilson, C. H. Woodall and P. R. Raithby, *Chemistry – A European Journal*, 2014, **20**, 3128-3134; b) S. E. Bajwa, T. E. Storr, L. E. Hatcher, T. J. Williams, C. G. Baumann, A. C. Whitwood, D. R. Allan, S. J. Teat, P. R. Raithby and I. J. S. Fairlamb, *Chemical Science*, 2012, **3**, 1656-1661.
11. Vorontsov, II, T. Graber, A. Y. Kovalevsky, I. V. Novozhilova, M. Gembicky, Y. S. Chen and P. Coppens, *J. Am. Chem. Soc.*, 2009, **131**, 6566-6573.
12. L. E. Hatcher and P. R. Raithby, *Coord. Chem. Rev.*, 2014, DOI: 10.1016/j.ccr.2014.02.021.
13. R. Wen, I. Bernal, F. Somoza, W. Li and F. R. Fronczek, *Inorg. Chim. Acta*, 1998, **282**, 96-109.
14. L. E. Hatcher, M. R. Warren, D. R. Allan, S. K. Brayshaw, A. L. Johnson, S. Fuertes, S. Schiffers, A. J. Stevenson, S. J. Teat, C. H. Woodall and P. R. Raithby, *Angew. Chem.-Int. Edit.*, 2011, **50**, 8371-8374.
15. D. Schaniel and T. Woike, *Phys. Chem. Chem. Phys.*, 2009, **11**, 4391-4395.
16. S. K. Brayshaw, J. W. Knight, P. R. Raithby, T. L. Savarese, S. Schiffers, S. J. Teat, J. E. Warren and M. R. Warren, *J. Appl. Crystallogr.*, 2010, **43**, 337-340.
17. M. A. Spackman and J. J. McKinnon, *CrystEngComm*, 2002, **4**, 378-392.
18. Y. Ohashi, *Crystallography Reviews*, 2013, **19**, 2-146.

19. C. F. Macrae, I. J. Bruno, J. A. Chisholm, P. R. Edgington, P. McCabe, E. Pidcock, L. Rodriguez-Monge, R. Taylor, J. van de Streek and P. A. Wood, J. Appl. Cryst.2008, **41**, 466-470.
20. M. D. Cohen and G. M. J. Schmidt, *Journal of the Chemical Society (Resumed)*, 1964, 1996-2000.
21. G. M. Sheldrick, *Acta Crystallogr. Sect. A*, 2008, **64**, 112-122.

Graphical Abstract

Thermal and Photochemical Control of Nitro-Nitrito Linkage Isomerism in Single-Crystals of [Ni(medpt)(NO_2)(η^2-ONO)]

L. E. Hatcher, E. J. Bigos, M. J. Bryant, E. M. MacCready, T. P. Robinson, L. K. Saunders, L. H. Thomas, C. M. Beavers, Simon J. Teat, Jeppe Christensen and Paul R. Raithby

In the single crystal [Ni(medpt)(NO_2)(η^2-ONO)] displays an equilibrium between the η^1-NO_2 and the η^1-ONO linkage isomers for one of the two independent molecules over the temperature range 150-298 K, and upon photoactivation at 100 K one of the η^1-NO_2 ligands converts to 89% of the η^1-ONO isomer and the other to 32%.